# POLITECNICO DI TORINO
## Repository ISTITUZIONALE

Nanoplastics Removal During Drinking Water Treatment: Laboratory- and Pilot-scale Experiments and Modeling

# Journal Pre-proof

Nanoplastics Removal During Drinking Water Treatment: Laboratory- and Pilot-scale Experiments and Modeling

Gerardo Pulido-Reyes, Leonardo Magherini, Carlo Bianco, Rajandrea Sethi, Urs von Gunten, Ralf Kaegi, Denise M. Mitrano

Please cite this article as: Gerardo Pulido-Reyes, Leonardo Magherini, Carlo Bianco, Rajandrea Sethi, Urs von Gunten, Ralf Kaegi and Denise M. Mitrano, Nanoplastics Removal During Drinking Water Treatment: Laboratory- and Pilot-scale Experiments and Modeling, *Journal of Hazardous Materials,* (2022) doi:https://doi.org/10.1016/j.jhazmat.2022.129011

This is a PDF file of an article that has undergone enhancements after acceptance, such as the addition of a cover page and metadata, and formatting for readability, but it is not yet the definitive version of record. This version will undergo additional copyediting, typesetting and review before it is published in its final form, but we are providing this version to give early visibility of the article. Please note that, during the production process, errors may be discovered which could affect the content, and all legal disclaimers that apply to the journal pertain.

# Nanoplastics removal during drinking water treatment: Laboratory- and pilot-scale experiments and modeling

Gerardo Pulido-Reyes[a,*, §], Leonardo Magherini[b], Carlo Bianco[b], Rajandrea Sethi[b], Urs von Gunten[a, c, d], Ralf Kaegi[a,*], Denise M. Mitrano[d].

[a]Eawag, Swiss Federal Institute of Aquatic Science and Technology, Ueberlandstrasse 133, 8600 Duebendorf, Switzerland.

[b]Department of Environmental, Land and Infrastructure Engineering, Politecnico di Torino, Corso Duca degli Abruzzi, 24, 10129 Turin, Italy

[c]School of Architecture, Civil, and Environmental Engineering (ENAC), École Polytechnique Fédérale de Lausanne, CH-1015, Lausanne, Switzerland.

[d]Environmental Systems Science Department, ETH Zurich, 8092, Zurich, Switzerland.

## Abstract

Microplastics detected in potable water sources and tap water have led to concerns about the efficacy of current drinking water treatment processes to remove these contaminants. It is hypothesized that drinking water resources contain nanoplastics (NPs), but the detection of NPs is challenging. We, therefore, used palladium (Pd)-labelled NPs to investigate the behavior and removal of NPs during conventional drinking water treatment processes including ozonation, sand and activated carbon filtration. Ozone doses typically applied in drinking water treatment plants (DWTPs) hardly affect the NPs transport in the subsequent filtration systems. Amongst the different filtration media, NP particles were most efficiently retained when aged (i.e. biofilm coated) sand was used with good agreements between laboratory and pilot scale systems. The removal of NPs through multiple filtration steps in a municipal full-scale DWTP was simulated using the MNMs software code. Removal efficiencies exceeding 3-log units were modeled for a combination of three consecutive filtration steps (rapid sand filtration, activated carbon filtration and slow sand filtration with 0.4-,

0.2- and 3.0-log-removal, respectively). According to the results from the model, the removal of NPs during slow sand filtration dominated the overall NPs removal which is also supported by the laboratory-scale and pilot-scale data. The results from this study can be used to estimate the NPs removal efficiency of typical DWTPs with similar water treatment chains.

*Keywords*: nanoplastics, drinking water treatment, ozonation, sand filtration, granular activated carbon.

§Current affiliation: Spanish National Institute for Agricultural and Food Research and Technology (INIA-CSIC). Crta. de la Coruña, km 7.5 - 28040 Madrid, Spain.

*Corresponding authors: Ralf Kaegi (ralf.kaegi@eawag.ch) and Gerardo Pulido-Reyes (gerardo.pulidoreyes@eawag.ch).

# 1 Introduction

Plastic pollution of water bodies is of global environmental concern. Plastic particles have been detected everywhere around the world, from wastewater to marine environments to freshwater systems [1, 2]. Microplastics (MPs, solid plastic particles with a diameter between 1 µm and 5 mm) have been reported in potable water sources, including tap and bottled water for human consumption [3]. Reports on the occurrence of nanoplastics (NPs, solid plastic particles < 1 µm; [4]) in aquatic environments are limited due to the lack of analytical methods to reliably detect NPs, especially in complex matrices. Results from laboratory-scale studies have shown that different types of plastics such as polystyrene, nylon or polyethylene terephthalate degrade to form NPs [5, 6]. It is, therefore, hypothesized that the degradation of larger plastic items generates microplastics which further degrade into NPs [7, 8]. Consequently, drinking water sources may already contain NPs, but the extent of contamination remains unknown to date.

The purpose of drinking water treatment plants (DWTPs) is to provide the public with safe water with a good hygienic and chemical quality [9]. This underlines the need to understand and assess the capacity of drinking water treatment processes to remove NPs. Key processes used in DWTPs to remove dissolved and particulate contaminants from source water include coagulation/flocculation, sedimentation, ozonation and filtration systems [10]. Depending on the origin of the source water, different configurations are applied to remove microbiological or chemical contaminants. Surface water typically requires a multi-barrier treatment [9] in contrast to groundwater, which often only requires limited treatments. Several studies reported MP removal efficiencies exceeding 85 % for current drinking water treatment chains [11-14]. However, due to the lack of standardized and validated sampling and measurement protocols, these results have to be interpreted with care. Studies focusing on MPs larger than 1 µm in DWTPs using surface waters as a drinking water source reported between a few hundred up to a thousand MP particles/L in the treated water [12, 13, 15]. However, considerably lower concentrations were reported in two other studies, targeting particles > 10 µm by filtration and using both groundwater and surface waters [11, 14]. These contrasting results may reflect the diversity of water sources, the different analytical approaches used, different modes of operation and compositions of filters and, most importantly, the different size detection limits of the analytical techniques used.

DWTP operational parameters including flow rate, filtration media and their surface properties as well as the water quality of the source water, govern the transport and deposition behaviors of particles in drinking water filtration systems [16]. The development of biofilms on filtration media has the potential to substantially reduce the transport of particles in saturated porous media [17, 18]. Although the transport and deposition of colloids (including NPs) in water saturated column experiments using various filtration media have been studied over the last decades [19-22], the transport

of NPs under typical conditions relevant for drinking water treatment has received less attention. Recent studies have pointed out that drinking water treatment may remove NPs from the source water and that the removal efficiency varies depending on the selected treatment processes [23-25]. Filtration processes seem to be effective in removing NPs, however how ozonation alters the subsequent filtration treatment has not been assessed yet. Thus, to guarantee and maintain the high standards of drinking water quality, it is necessary to assess to what extent current drinking water processes remove NPs from the feed water.

The aim of this study was to investigate the physicochemical changes and the behavior of NPs during processes relevant for drinking water treatment, including ozonation and sand and AC filtration. To overcome the challenges associated with the detection of NPs in complex matrices, we used metal (Pd)-doped NPs, which allowed for the quantification of the NPs by utilizing an inorganic tracer [26-28]. Thanks to this approach, trace concentrations of NPs can be accurately tracked and measured, providing robust data to the existing literature of NPs removal in DWTPs [23-25]. Batch experiments were conducted to evaluate the impact of typical ozone doses applied during drinking water treatment on the physicochemical properties of the NPs, including assessing the leaching potential of the Pd tracer from the NPs. Transport studies using columns filled with pristine or aged (i.e. biofilm covered) sand or AC were performed to assess the effectiveness of the media filtration to remove NPs. The impact of flow rate on NPs removal was evaluated using columns packed with pristine sand at two different flow rates, mimicking slow and rapid sand filtration. To assess the scalability of the results beyond laboratory-scale studies, additional experiments were conducted on sand and AC filtration units of a pilot-scale DWTP operated with Lake Zurich water. We measured breakthrough curves of NPs through both the columns and pilot-scale filters under different conditions (e.g. flow rate, filter bed depth) to elucidate the impact of the different processes on NP retention. The Micro- and Nano-particles transport, filtration

and clogging Model Suite (MNMs software [29, 30] was used to model the breakthrough curves obtained from the pilot-scale filtration experiments and to derive the hydrodynamic parameters of the filtration systems. A comparison between results from the model and the experimental data allowed us to identify the mechanisms driving the physicochemical interactions between NPs and the filtration media and to estimate the kinetic parameters governing particle filtration. Based on these results, we simulated the behavior of NPs in different media filtration systems of a full-scale DWTP, including rapid and slow sand filtration and AC filtration processes, taking into account the biofilm on the filtration media. This resulted in a prediction of NP removal in terms of relative NP removal efficiency, total retained mass, and NP concentrations in the finished water.

## 2 Materials and methods

### 2.1 Metal-labelled nanoplastics

NPs were synthesized and characterized as previously described [27]. Briefly, the particles had a core/shell structure with a polyacrylonitrile core doped with palladium (Pd) and a polystyrene shell. Two synthesis batches were used in this study, resulting in core/shell NPs with similar physicochemical properties. Hydrodynamic diameter and ζ-potential of the NPs were calculated from dynamic light scattering (DLS) and electrophoretic light scattering (ELS) measurements, respectively (Zetasizer NanoZS, Malvern Instruments Ltd., UK). Particles derived from the first synthesis batch (SB1) were used for the laboratory studies and had a hydrodynamic diameter (Z-average) of 214.7 nm ± 1.4 nm (polydispersity index: 0.07) and ζ-potential of -41.1 mV ± 0.3 mV measured in ultra-purified deionized water (DI water, pH 6.8, NANOpure Diamond purification system, Thermo Fisher Scientific, 18.2 MΩ-cm). The second synthesis batch (SB2), used for pilot plant experiments, resulted in NPs with a hydrodynamic diameter of 163.5 nm ± 0.3 nm (polydispersity index: 0.03) and ζ-potential of -45.7 ± 0.8 mV in DI water (pH 6.9). Characterization of the NPs using scanning transmission electron microscopy (STEM) along with information on the operational parameters of the microscopes is provided in the supporting information (SI) (Figure S1). All NPs were stored at room temperature in the dark until used.

### 2.2 Feed water and filtration media characterization

DI water and Lake Zurich water (source of drinking water for the city of Zurich, Switzerland) were used for the preparation of NP suspensions. Lake water was collected at a depth of 30 m from the inlet of a Lake Zurich DWTP (WVZ-Lengg) and filtered through a 0.45 μm filter (cellulose membrane filter, Whatman®). Physicochemical properties of the lake water are provided in Table S1. Pristine and aged sand and AC were used as media for filtration experiments. Pristine refers to

media that has not been previously used in a DWTP and aged refers to media which was collected from the top of the rapid sand and AC filters of a lake water pilot plant (WVZ-Lengg), which has been in continuous operation since 2007 [31]. The grain size distribution of the pristine sand (Carlo Bernasconi AG, Switzerland) and AC (Chemviron F400, Brussels, Belgium) and their aged analogues were measured using static light scattering (LS 13 320 model, Beckman Coulter, USA). The mean diameter for the pristine and aged sand was 450 µm. Pristine and aged AC had a mean diameter of 1050 and 950 µm, respectively (Fig. S2. The uniformity coefficient ranged between 1.71 and 1.78 for all filtration media (Table S2). Surface area measurements of the different filtration media were carried out by $N_2$ adsorption–desorption isotherms at 77 K using a surface area analyzer (QuantaChrome Nova 1200) with substrates previously dried at 100 ºC during 4 h. The BET surface area was calculated by QuantaChrome™ NovaWin software using the Brunauer–Emmett–Teller (BET) equation in a relative pressure range of $P/P_0$ = 0.050–0.125. The surface area of pristine sand and AC was 0.58 and 857.37 $m^2/g$, and 0.21 and 225.38 $m^2/g$ were measured for the aged sand and AC, respectively (Table S3).

*2.3 Inductively coupled plasma – mass spectrometry (ICP-MS) analysis of NPs*

Pd concentrations in the NP stock suspensions and in suspensions from laboratory- and pilot-scale experiments were measured by ICP-MS (8900 ICP-MS Triple Quad or 7500 ICP-MS, Agilent Technologies), using indium as an internal standard. Pd ICP-MS calibration solutions (Pd standard for ICP-MS, 10 000 mg/L, Sigma-Aldrich) ranging from 0.05 to 10 µg/L were prepared daily in 2% nitric acid (Rotipuran Supra 69%, Carl Roth, Germany). To assess the NP recovery in the different matrices used in this study, NPs were directly spiked in DI water, lake water, sand and AC powder. Average recovery of Pd over all tested concentrations and matrices was 98.1 % ± 1.8 (Table S4). Plastics which were spiked in aqueous matrices (DI and lake water) were directly injected into to ICP-MS, whereas solid samples containing NPs (sand and AC) were

acid digested following the protocol described in [26]. For this, hydrogen peroxide (1.5 mL, $H_2O_2$, >30%, Sigma Aldrich), nitric acid (6 mL, $HNO_3$, 65%, Merck) and sulfuric acid (0.25 mL, $H_2SO_4$, 95-98%, Sigma Aldrich) were used. Sample digestion was performed in a microwave assisted acid digestion system (ultra-CLAVE 4, MLS GmbH) operated at a pressure of 120 bar and at 250 ºC for 10 min. Digestion tubes and caps were made of Teflon, with sample volumes of 9 mL. The digestion protocol was optimized to digest both particulate plastic and organic matter in the samples. First, 1.5 mL $H_2O_2$ was added to the sample directly in the digestion tube. Second, 6 mL $HNO_3$ was added and the sample was stored for 30 min before 0.25 mL $H_2SO_4$ was added and the samples were loaded into the microwave system. After digestion, the samples were quantitatively transferred to polypropylene Falcon tubes, filled with DI water to a volume of 50 mL and the content of Pd was measured by ICP-MS. Initially, $^{105}Pd$ was the isotope selected for quantification, however, polyatomic interferences with $SrOH^+$ were observed in experiments conducted with lake water. Therefore, the Pd signal was corrected for the offset due to $SrOH^+$. This issue was circumvented for pilot experiments by measuring $^{106}Pd$ and $^{108}Pd$ isotopes instead, where polyatomic interferences were not observed.

*2.4 Laboratory-scale experiments*

*2.4.1 Ozonation*

NPs were suspended in lake water at a concentration of 1.7 mg/L (equivalent to 5.5 µg Pd/L or $1.7 \cdot 10^{12}$ particles/L). Ozone stock solutions (1.15 mM) were produced by continuously bubbling an ozone/oxygen gas mixture into ice-cooled DI water [32]. The ozone concentration in the stock solution was measured spectrophotometrically at 258 nm ($\varepsilon = 3200$ $M^{-1}$ $cm^{-1}$) [33]. NPs were treated with three ozone doses (0.5, 1 and 5 mg/L) for a total time of 45 min, representing both realistic and high ozone doses and exposures used in drinking water treatment [34]. Ozonation was performed in absence of a hydroxyl radical scavenger to allow both ozone and hydroxyl radical reactions [33].

The hydrodynamic diameter and ζ-potential of the particles in suspension before and after the ozone treatment were measured by DLS and ELS, respectively. To quantify the free Pd in solution before and after ozonation, the suspensions were passed through a centrifugal ultrafilter (Vivaspin 2) with a 50 kDa MWCO cutoff (Sartorius AG, Goettingen, Germany) and the Pd concentrations in the filtrates were determined by ICP-MS. Changes in the morphology of the NPs were assessed by STEM.

*2.4.2 Laboratory column filtration experiments*

Column experiments were performed at room temperature in triplicate using glass columns (5 cm inner diameter and height adjustable end-pieces (Diba Industries Inc., USA)). Pristine and aged sand and AC were used as filtration media. The glass columns were packed with the filtration media as described in [35]. The columns were saturated with DI water and injected in an up-flow mode to remove any entrapped air. To preserve the surface characteristics of the filtration media, the aged substrates were wet packed. A layer of glass fiber wool (Sigma-Aldrich) was placed at the bottom and top of all columns to prevent any loss of sand or AC.

Once saturated, the system was conditioned by introducing DI or lake water at 5 mL/min for four pore volumes (one pore volume ranged between 20 to 169 mL depending on the length of the column) using a Cheminert® M50 pump (Valco Instruments, USA). Subsequently, either a spike of a dissolved tracer (0.01 M NaCl) or a NP suspension at 1.7 mg NPs/L was injected into the column, followed by flushing with several pore volumes of DI or lake water. Following the same procedure, tracer tests with NaCl (Fig. S3) were performed by measuring the electrical conductivity at the effluent of the column with a ζ-potential flow cell connected to the Zetasizer Nano ZS. The pore volume was calculated using NaCl as described in [36]. Breakthrough curves (BTCs) of NPs were obtained by plotting the effluent concentration of Pd as a tracer for the NPs normalized by the concentration in the feed suspension ($C/C_0$) as a function of

9

the filtered water expressed in pore volumes. To evaluate the potential loss of NPs due to attachment to the tubing, within the pumps, or to the glass fiber filters, a column packed with glass beads (1 mm diameter; SILIBeads Type M, Sigmund Lindner, Germany) was used as a control. The breakthrough curves of NPs showed complete recovery, demonstrating particle losses within the experimental system were negligible (Fig. S4).

Different filter lengths and flow rates were evaluated in a set of column experiments. Pristine sand was packed in columns with lengths of 2, 11.5 and 20 cm. The flow rates at which the NPs were injected were set at either 5 mL/min (0.28 m/h) or 21 mL/min (1.02 m/h), mimicking slow and rapid sand filtration, respectively, although 21 mL/min (1.02 m/h) is at the lower limit for rapid sand filtration [37, 38]. Although slow sand filters typically use sand with different mean diameters, here only the flow rate has been modified to limit the complexity of the experiments. The impact of the filtration media (sand and AC), its surface properties in terms of age (pristine and aged media) and of the feed water type (DI or lake water) on the transport of NPs was evaluated at a fixed filter length of 11.5 cm and a flow rate of 5 mL/min. To assess whether ozonation influenced the transport of NPs through the filtration media, additional filtration experiments were conducted with NPs that have been pre-treated with an ozone dose of 1 mg/L. All experimental conditions for the column experiments are provided in Table S5.

### 2.4.3 Pilot plant experiments

Pilot-scale filtration experiments were conducted at the Zurich Water Works (WVZ-Lengg, Zurich, Switzerland). Two identical filter columns for rapid sand and AC filtration were operated in down-flow mode. Each column had a diameter of 1.1 m and a total height of 2.65 m, where the height of the filter bed was 1.85 m. The space above the filter bed was filled with water. Each column had 8 ports for collecting water samples:

one located 0.1 m above the filter bed surface; 6 at different depths along the filter bed (0.1, 0.2, 0.3, 0.6, 0.9 and 1.4 m from the top of the filter bed) and one at the filter outlet. At the end of the experiment, solid samples from the filter beds were collected from five depths (0.10, 0.40, 0.75, 1.10 and 1.45 m from top of the filter bed). A scheme and a photograph of the pilot plant is provided in Figure S5.

NPs (141.6 mg/L; 0.5 mg Pd/L) were injected with a pump (12 L/h; Delta Optodrive, ProMinent S.A.) into the pipe which delivered the lake water to the pilot plant at 6 °C (pH 7.9). The concentration of NPs in the water above the filter beds was adjusted to the same concentration as in the laboratory filtration experiments (i.e., 1.7 mg NPs/L). Despite the lower NP concentrations currently expected in drinking water sources, such a high NP concentration was selected to mimic an accelerated aging of the pilot-scale filters and to ensure a robust quantification of NP concentrations even at the system outlet. The pilot plant experiments were initiated by injecting NPs for 6.3 h followed by 2.7 h of NPs-free lake water, maintaining a flow rate of 1 $m^3$/h in each filter tank (Darcy velocity: 1.05 m/h) during the entire experimental period. This injection schedule was chosen to allow for a feasible experimental protocol which included preparation, sampling and post-treatment during a working day. The flow rate of 1 $m^3$/h corresponds to the highest flow rate in the laboratory filtration experiments (rapid sand filtration). Water samples were collected in 15 mL polypropylene tubes from the seven sampling points located at the side of the filters as well as at the outlet of the filter every 20 min over the course of 9 h. Breakthrough curves of NPs were obtained by plotting the effluent concentration of Pd as a tracer for the NPs normalized by the initial concentration ($C/C_0$) as a function of the filtered water expressed as pore volume. Once the experiment was completed, the water flow was stopped and a metal tube (inner and outer diameter of 0.9 and 1.1 cm, respectively) was inserted into the filters through sampling ports located on the side walls of the filters to collect the solid filter media samples. Approximately 20 g of AC and 45 g of sand was collected from each

sampling point and dried at 100 ºC for 24h. Subsequently, triplicate samples of 35 mg of each substrate were weighed and acid digested as described above.

To estimate the pore volume in each filter, an inert tracer experiment was conducted using NaCl (data not shown). A concentrated NaCl solution was fed into the incoming lake water to reach a concentration of 3.9 mM. The tracer was injected for 3 h followed by 2.5 h of flushing with a tracer-free period. Conductivity was measured with three conductivity meters (Multi3430 IDS, MultiLine, WTW, Germany) at three different ports every 10 min: at 0.10 m above the surface filter, at 0.90 m depth and at the outlet. An estimate of the pore volume for each filter was determined based on the breakthrough curves following the same procedure as described for column experiments. Moreover, the porosity and dispersivity of each filtration column were estimated by least-squares fitting of the experimental breakthrough curves using the MNMs software code (www.polito.it/groundwater/software). The estimated porosity was 0.45 for both filters. The estimated dispersivities were 3.1 cm for the sand and 5.2 cm for the AC, which correspond to dispersion coefficients of $2.01 \cdot 10^{-5}$ m$^2$/s and $3.37 \cdot 10^{-5}$ m$^2$/s, respectively.

*2.5 Modeling filtration of NPs*

*2.5.1 Transport model for NPs*

NP transport in a mono-dimensional porous medium can be modelled by the following modified advection-dispersion equation that describes the dual-phase interactions between liquid and solid phase [39, 40]:

$$\begin{cases} \dfrac{\partial}{\partial t}(\epsilon C) + \sum_i \dfrac{\partial}{\partial t}(\rho_b S_i) + \dfrac{\partial}{\partial x}(q_x C) - \dfrac{\partial^2}{\partial x^2}(\epsilon D C) = 0 \\ \dfrac{\partial}{\partial t}(\rho_b S_i) = \epsilon k_{a,i} f_{att,i} C \end{cases} \qquad Eq.\ 1$$

where $\epsilon$ is the effective porosity of the porous medium $(-)$, $\rho_b$ is the bulk density $(kg\ m^{-3})$, $D$ is the dispersion coefficient $(m^2\ s^{-1})$, $q_x$ is the Darcy flow velocity $(m\ s^{-1})$, $C$ is the concentration of particles suspended in liquid phase $(kg\ m^{-3})$, $S$ is the concentration of particles retained on the filter medium $(kg\ kg^{-1})$ and $k_{a,i}$ is the attachment coefficient $(s^{-1})$ that regulates the rate of particle deposition. $f_{att,i}$ is a generic function that can assume different formulations based on the case-specific physicochemical mechanism governing the NPs-filter interactions. The subscript $i$ refers to the possibility to have more than one concurrent interaction mechanism.

When the NPs concentration and the ionic strength of the suspension are low, the attachment coefficient $k_a$ can be expressed as a function of the single collector contact efficiency, $\eta_0$, and of the attachment efficiency, $\alpha$ [41, 42]:

$$k_{a,i} = \frac{3(1-\epsilon)}{2\epsilon d_{50}}\alpha q_x \eta_0 \qquad\qquad Eq.\ 2$$

where $d_{50}$ is the average grain diameter of the filter medium (m). The finite difference numerical model MNMs 2021 was used to solve the system of partial differential equations reported in Eq. 1.

### 2.5.2 Modeling of the pilot-scale filtration units

Each pilot filtration experiment was modelled using the *MNMs* 2021 software. The filtration bed models were built following the geometry and operating conditions of the pilot plant described above. The filter depth was divided into 1000 cells perpendicular to the flow direction, where a 100 s time step was chosen for time discretization. Porosity and dispersivity were determined by reverse fitting of the NaCl tracer test results.

The experimental breakthrough curves from all the intermediate sampling ports and from the filter outlet were fitted simultaneously using the Levenberg-Marquardt method for non-linear least-squares. Experimental data fitting allowed identification of the main retention mechanisms governing the case-specific NPs-filter interactions and to estimate the corresponding attachment coefficients. The attachment efficiency was then calculated using Eq. 2, where the single collector contact efficiency $\eta_{MMS}$ was computed using the formulation proposed by [42].

*2.5.3 Long-term prediction for the pilot-scale filtration unit*

The model-based interpretation of the pilot-scale results provides information about the short-term NP filtration behavior, i.e. after less than 10 pore volumes. However, if the long-term filtration performances of a full-scale DWTP needs to be estimated, much longer operational times have to be considered. Therefore, the NP transport model used to predict the long-term filter behavior must also take into account later stage deposition processes, such as filter clogging, saturation, or blocking. Filter clogging occurs when a large quantity of particles is attached to the porous medium surface due to mechanical mechanisms or attractive particle-particle interaction forces (multilayer deposition). Clogging results in an increase of the filter efficiency, but also in a progressive reduction of the filter permeability and in the corresponding increase of the operational head losses. Filter saturation conversely occurs when particle-particle interactions are repulsive and only single-layer particle deposition is possible within the porous medium. In such cases, a progressive reduction of the filter removal efficiency would be observed until full coverage of the porous medium surface available for NPs deposition is achieved (i.e. blocking mechanism). Due to the physical properties of NPs, i.e. small size and negative surface charge in lake water, the more conservative filter saturation scenario was considered in this study. From a mathematical point of

view, the filter saturation is simulated applying the equation system described in Eq. 13, where the generic attachment function $f_{att,i}$ is modelled as a blocking function:

$$f_{att,i} = 1 - \frac{S_i}{S_{max}}$$ 

*Eq. 3*

where $S_{max}$ is the maximum saturation concentration $(kg/kg)$. $S_{max}$ was calculated as a fraction of the total specific surface area of the filter medium, according to equation 4:

$$S_{max} = 4\frac{m_p}{\pi d_p^2}\theta A_S$$ 

*Eq. 4*

where $\theta$ $(-)$ is the fraction of the solid surface area that is available for deposition, $m_p$ is the particle mass (kg), $d_p$ is the particle diameter $(m)$ and $A_S$ is the BET surface area $(m^2/kg)$. $\theta$ depends on the particle size, particle $\zeta$-potential, flow velocity and water chemistry [43]. For polystyrene particles and water quality conditions similar to those considered in this study, $\theta$ values range from 1% to 5% [43, 44]. Hence, 1% was selected as a conservative estimate. The $A_S$ value for AC is much higher than for sand due to the presence of microporosity. However, the size of AC micropores is usually lower than 50 nm and therefore, it has been assumed that the NPs cannot access the micropores (the diameters of the NPs used in this study were > 100 nm). The $A_S$ accessible to particles for AC (only the external surface) was set equal to the value for sand (sand and AC have similar grain sizes and uniformity coefficients). Although this assumption underestimates the contribution of the AC macroporosity and surface roughness for plastics deposition, it guarantees a more conservative prediction of the long-term behavior of the filter. Therefore, for both filter media, $S_{max}$ were equal to $2.61 \cdot 10^{-4}\ kg/kg$, assuming $m_p$, $d_P$ and $A_S$ respectively equal to $2.61 \cdot 10^{-18}\ kg$, $1.64 \cdot 10^{-7}\ m$ and $210\ m^2/kg$. Since the blocking dynamics are sensitive to the particle concentration entering the system during the overall filter operational time, and since the NP concentration in drinking water sources is unknown, simulations for both AC and sand filters were run considering different inlet NP concentrations (2, 0.2, 0.02

mg/L). The results are expressed as the time (in days) necessary to reach removal percentages from 99 % to 0 % (full saturation).

### 2.5.4 Simulation of a drinking water treatment plant

The removal of NPs in a full-scale drinking water treatment plant was simulated. The model plant considered in this study is based on a lake DWTP (Zurich), which produces 40% of the drinking water for the city by treating Lake Zurich water. The treatment consists of (1) pre-ozonation; (2) rapid sand filtration (80 cm of quartz sand); (3) intermediate ozonation; (4) AC filtration (double layer filter with 130 cm of AC and 40 cm of quartz sand) and (5) slow sand filtration (100 cm of quartz sand) [34]. Although each filtration step consists of 12-38 filters operated in parallel in the DWTP, only one filter unit of each step was considered for the simulations. Additional layers typically present in real treatment plants, such as pumice or gravel strata, were not considered here since their contribution to NP filtration were expected to be negligible. The results from the pilot plant filtration experiments and the information extracted thereof (attachment coefficients and retention mechanisms) were used for the simulation of NPs removal in the full-scale DWTP. The same attachment coefficient were used for the slow and rapid sand filtration units as comparable values were obtained from the pilot experiments ($k_a$ = 0.0025 s$^{-1}$) at high flow rate and from the column filtration experiments ($k_a$ = 0.0030 s$^{-1}$) performed with analogous conditions (lake water and aged sand) with the slow flow rate (Fig. S6).

Three different flow rates simulating the minimum, average and maximum flows applied in the full-scale plant for each filtration step were considered to assess the influence of this parameter on the DWTP performance. Flow rates of 1.2, 3 and 6 m/h were simulated for the rapid sand filtration (the latter one being the most representative in DWTP), 4.3, 13 and 21 m/h for the AC filtration and 0.25, 0.48 and 0.70 m/h for the

slow sand filtration. An inlet NP concentration (2 mg NPs/L) was imposed to be similar to the inlet concentration used during the column and pilot experiments. The output data are expressed as mass of NPs. The DWTP filtration steps were simulated to predict the removal efficiencies, $\eta$, and the $\log_{10}$ removal, $LRV$, for both the individual filters and the overall treatment. The following relationships were used to estimate the removal efficiency, $\eta$, (Eq. 5) and the $\log_{10}$ removal, $LRV$ (Eq. 6):

$$\eta = 1 - \frac{C_{OUT}}{C_{IN}} \qquad \text{Eq. 5}$$

$$LRV = \log_{10}\frac{C_{IN}}{C_{OUT}} \qquad \text{Eq. 6}$$

### 2.6 Statistical Analysis

The mean and standard deviation of the hydrodynamic diameter and surface charge from ozonation experiments were calculated for each treatment from three independent replicates. Statistical analyses were performed by using the R software 3.0.2 (The R Foundation for Statistical Computing©). One-way ANOVA coupled with Tukey's HSD (honestly significant difference) post hoc test was performed for comparison of means. Statistically significant differences were considered to exist when $p < 0.05$.

# 3 Results and Discussion

## 3.1 Effects of ozonation on NPs

The hydrodynamic diameter of the pristine NPs and of the NPs treated with variable ozone doses were similar (Fig. 1A), demonstrating that ozonation did not result in fragmentation or agglomeration of the NPs. However, the surface charge of the particles decreased with increasing ozone doses (Fig. 1B). The ζ-potential of NPs in lake water decreased from -11.1 mV (control in lake water) to -13.9, -15.0 and -16.5 mV after pre-treatment with 0.5, 1 and 5 mg $O_3$/L, respectively. It is noteworthy that the particle surface charge decreased using ozone doses typically applied in DWTP, i.e. as low as 0.5 mg $O_3$/L. This effect was also found for polystyrene NPs that were treated with $O_3$, and can be explained by a surface oxidation of the exposed particles potentially leading to carboxylic type functional groups [33, 45].

To assess if the ozone treatment also altered the surface structure of the NPs, secondary electron images were obtained from pristine particles and particles exposed to 5 mg $O_3$/L (Fig. 1C and 1D). A similar size and surface structure for pristine and ozone-treated particles was observed, suggesting that ozone doses of 5 mg $O_3$/L did not result in the formation of cracks on the particle surface. In all experiments, the Pd concentrations measured in the filtered solutions was 0.044 ± 0.004 µg/L, corresponding to approximately 0.6 % of the total Pd content for both treated and untreated samples (Fig. S7). This indicates that the Pd-tracer remained within the NPs during the ozone treatments.

The ozone treatment resulted in a statistically significant decrease of the ζ-potential of the particles. However, the observed decrease of less than 7 mV is unlikely to impact the behavior of the ozone-treated NPs in further filtration experiments. Several studies have previously exposed polystyrene surfaces to ozone for different purposes such as the introduction of surface modifications for enhancing cell adhesion or biodegradation

[46-48]. It was reported that ozone effectively induced different alterations, including an increase in the material hydrophilicity and surface oxidation with an increase of carbonyl, epoxy and hydroxyl groups. However, the ozone doses in previous experiments were either much higher (up to 120 mg $O_3$/L) and the experiments were conducted over extended periods of time (up to 3h), or the surfaces were directly exposed to ozone in the gas phase [46-48]. Therefore, the results from these studies are difficult to compare to our data directly, which approximated more realistic operational conditions in DWTPs.
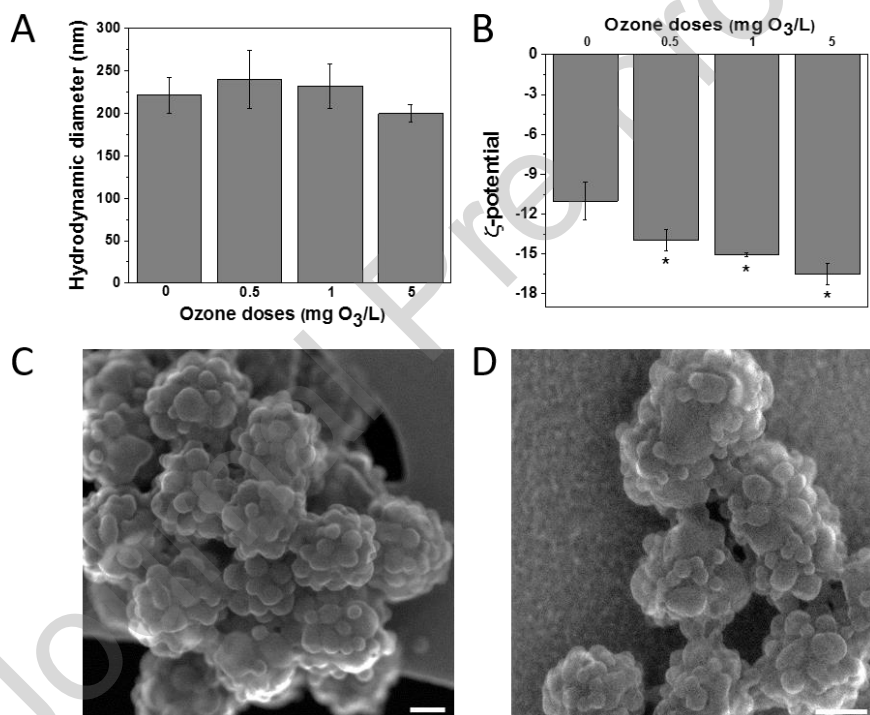


**Figure 1.** (A) Hydrodynamic diameter and (B) ζ-potential of NPs after exposure to ozone in lake water at 0 (control), 0.5, 1 and 5 mg $O_3$/L (pH 7.9). Statistically significant differences ($p < 0.05$) are marked by asterisks. Error bars indicate the standard deviations of triplicate experimental replicates. The impact of other particles in the lake water on the hydrodynamic diameter and ζ-potential is expected to be negligible. Secondary electron images of NPs (C) untreated and (D) treated with 5 mg $O_3$/L in lake water. Scale bar: 100 nm.

*3.2 Retention of NPs during filtration experiments in laboratory-scale studies*

Filtration experiments using sand columns were conducted to assess the role of flow rate and filter length on the transport of NPs through sand filtration media (Fig. 2). Increasing filter lengths and decreasing flow rates both increased the retention of NPs in the columns. This is due to the increased NPs residence time in the column resulting in a higher probability for particle-filtration media interactions, e.g., NPs deposition on the filtration media. The maximum NPs fraction recovered in the effluent at a flow rate of 0.28 m/h for the 2, 11.5 and 20 cm long filters was equal to 78%, 57% and 40% of the injected NP concentration. This means that depending on the flow conditions, between 22% and 60% of the NPs were retained in the column. When the flow rate was increased, a lower NP retention in the column was observed for all column lengths. This trend can be explained by the shorter residence time of the NPs in the columns and by the increased drag forces acting on the NPs, both reducing the probability for particle deposition and thus increasing their mobility in the sand columns. Similar observations were also reported from filtration studies using engineered nanoparticles [49, 50]. Therefore, we expect an efficient removal of the NPs in the slow sand filters, which can be further enhanced by increasing the filter depth.
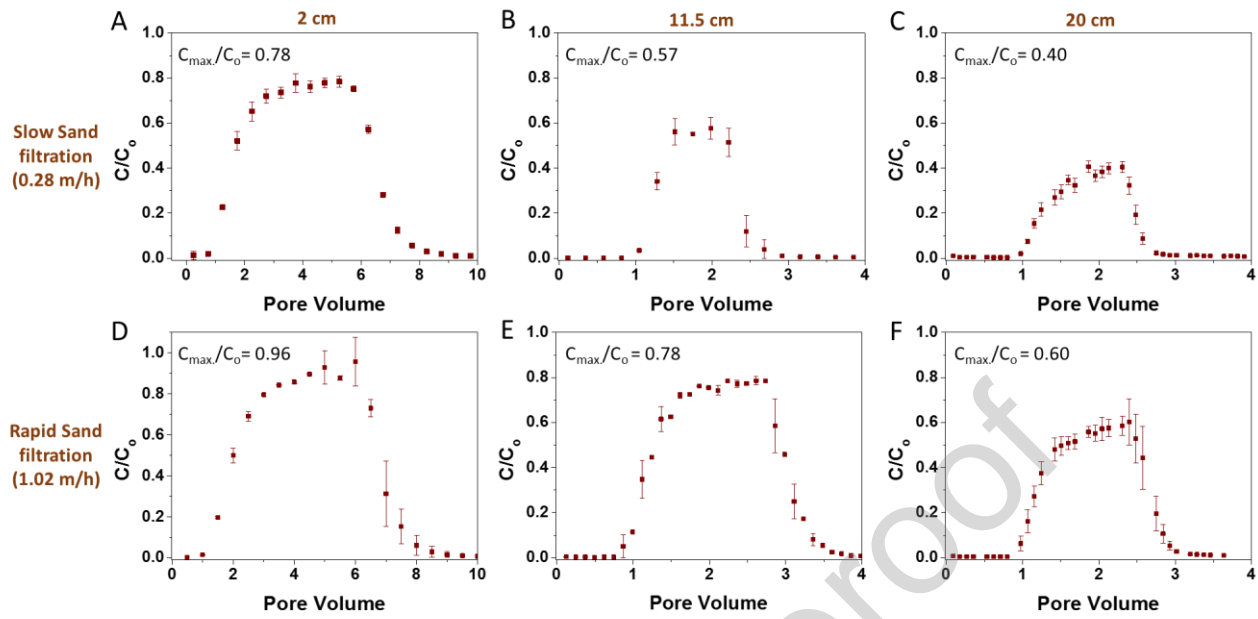
**Figure 2.** Impact of flow rates (0.28 m/h, A-C, and 1.02 m/h, D-F) and filter length (2, 11.5 and 20 cm) on particle transport in sand columns. $C_o$: NP concentration in the feed suspension, C: NP concentration in the column effluent, $C_{max}$: maximum concentration in the column effluent. Error bars represent standard deviations from triplicate experiments.

After assessing the influence of column length and flow rate, the impact of the filtration media type (sand and AC), surface characteristics (pristine and aged substrates) and type of feed water (DI or lake water) on NP transport was evaluated using a fixed column length (11.5 cm) and a flow rate of 0.28 m/h (Fig. 3). Experiments conducted with DI water and pristine sand and AC as filtration media showed $C_{max}/C_0$ values of 57% and 21%, respectively (Fig. 3A and 3B). The use of aged media collected from filters of the pilot-scale DWTP reduced $C_{max}/C_0$ values for the sand but increased $C_{max}/C_0$ values for AC. The increased NP retention (decreased $C_{max}/C_0$) in the aged sand ($C_{max}/C_0$ of 23%, Fig. 3C) compared to the pristine sand ($C_{max}/C_0$ of 57%, Fig. 3A) can be explained by the presence of a biofilm on the sand surfaces, modifying the surface properties of the filtration medium and, thus, leading to enhanced NP retention. Biofilm coatings are known to reduce particle mobility by (i) inducing a neutralization of

21

the surface charge of the filtration medium, (ii) producing surface charge heterogeneities, (iii) increasing the porous medium surface roughness and (iv) modifying the pore geometry [51, 52]. An enhanced retention due to the biofilm has also been observed in previous studies with different engineered nanoparticles [17, 50-52]. In contrast to what was observed in experiments conducted with the pristine and aged sand as filtration media, NP retention decreased when aged AC was used as filtration media. Nearly two thirds of the NPs passed the aged AC filtration media (Fig. 3D). This reduced NP retention in aged AC may be explained by a physical alteration of the individual AC grains. The complex and multiscale pore structure of AC, containing pores at varying scales from 50 µm to less than 1 nm, provides an ideal surface for the deposition and thus retention of particulate materials. Conversely, organic matter from the Lake Zurich water may have clogged AC pores [53] and subsequently reduced the surface area available for particle deposition. Based on BET measurements (Table S3), pristine AC had a surface area of 857 m²/g, but the aged AC had a considerably lower value (225 m²/g), which may be an indication of the loss of available surface area for particle deposition.

The opposite trends for NP retention observed for pristine and aged sand versus AC (Fig. 3A-D) may be explained by the aforementioned loss of available pores in AC grains, but also by the formation of different types of biofilms on the different filtration media and the different grain size distributions of aged sand and AC (Fig. S2). The type of filtration media determines the microbial communities associated with the developing biofilms, and different types of biofilm have been reported on different filtration media [54, 55]. It has, for example, been demonstrated that surface characteristics of biofilms with different degrees of hydrophobicity influence the transport of polystyrene NPs [19].

The type of feed water also impacted NP transport in aged filter media. The effect was most pronounced for aged sand media (Fig. 3C and 3E). $C_{max}/C_0$ values decreased by 19% and 6% for aged sand and AC (Fig. 3C-3F), respectively, when lake water was

used instead of DI water, and a nearly complete deposition of NPs within the aged sand media was observed. The reduced transport when using lake water was likely related to the increased ionic strength (2.53 mM and 0.04 mM for lake and DI water, respectively), leading to a compression of the electric double layer of both the NPs and the filtration media, favoring particle deposition. Similar trend and mechanism can be expected with pristine filtration media and lake water. This is in agreement with previous reports, highlighting the importance of DLVO-type interactions in the transport and deposition of different metal oxide [56-58] and polystyrene [44, 59] nanoparticles.

Drinking water treatment often includes an ozonation step followed by a post-filtration process. Pretreating the NPs with ozone before injection into the columns had only a minor impact on NPs transport, which is illustrated by the similar breakthrough curves for the ozonated and pristine NPs (Fig. 3E-H). In contrast, Liu et al. (2019) [45] reported an increase in the NP transport in sand columns with ozonated polystyrene nanoparticles, but NPs were exposed to an ozone dose of 36 g/L, resulting in particles with a high degree of hydrophilicity and highly negative ζ-potential (approximately - 50 mV compared to -16 mV with a dose of 5 mg/L in this study). The authors concluded that these properties facilitated the transport of NPs in the porous media. However, the ozone doses typically applied during drinking water ozonation range between 0.5 to 1.5 mg $O_3$/L ($\approx$ 1 mg $O_3$/mg DOC) [60]. Therefore, at ozone doses relevant for drinking water treatment, only negligible impacts on the retention of NPs during subsequent filtration steps are expected.
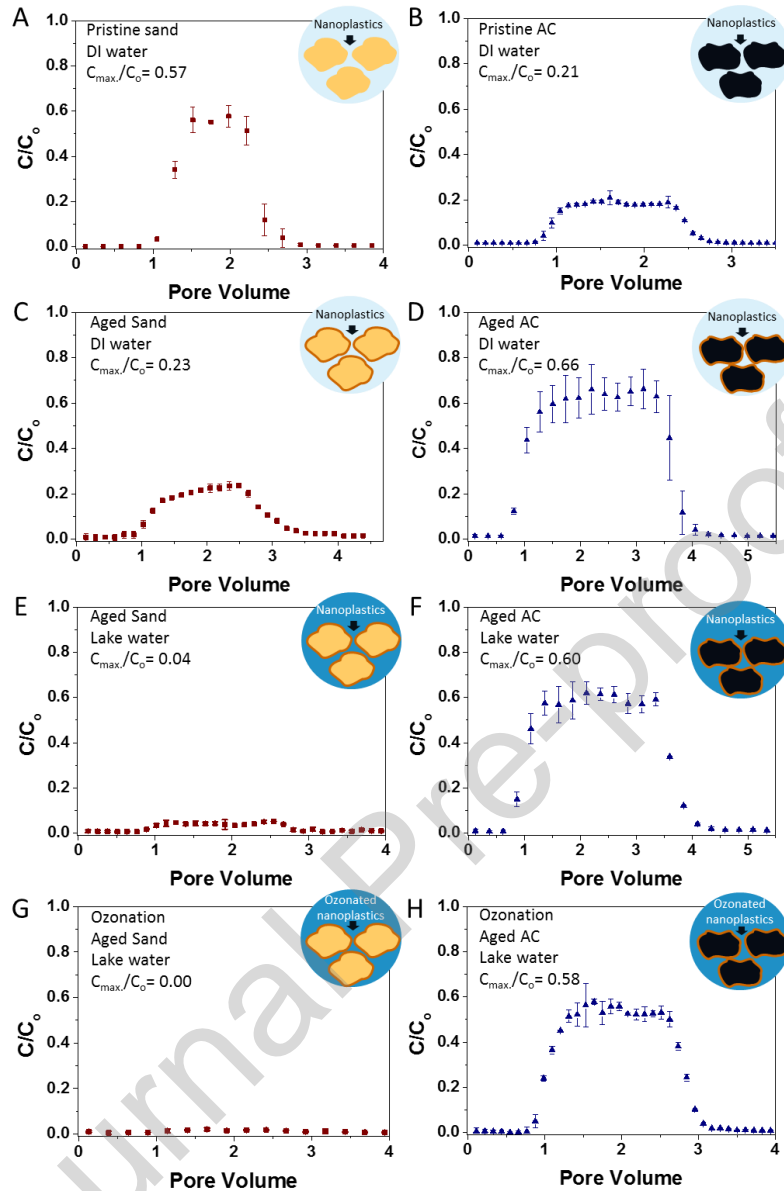
**Figure 3.** Influence of filter age (pristine or aged), filtration media (sand or activated carbon),and feed water (DI water or lake water) on the transport / retention of pristine and ozone-treated (1 mg/L) NPs. Error bars represent standard deviations from triplicate experiments.

## 3.3 Retention of NPs in pilot-scale filtration

### 3.3.1 Experimental data

The transport of NPs in pilot sand and AC media filtration units were assessed based on spiking experiments conducted over an experimental run time of 9 h (Fig. 4). NPs in the pilot filtration units were efficiently retained in the sand filter but showed less

retention in the AC filter, in agreement with the results from the laboratory-scale experiments. The retention of the NPs gradually increased with increasing the AC filter length (Fig. 4A), showing a plateau in all breakthrough curves. In the sand filtration unit, a high NP retention was observed in the first layers of the sand bed (Fig. 4C). 70% of the NPs were retained in the first 0.1 m of the sand filter and the retention further increased to 99.5% at 0.9 m. We observed that the outlet concentration of NPs in the uppermost sampling ports of the filter bed (0.1, 0.2 and 0.3 m) clearly increased over time (see Fig. 4C, insert), which may be caused by NPs being deposited on the sand grains and hampering the attachment of additional particles over time [61]. Experimental breakthrough curves for both filter types did not show significant tailing during the NP-free flushing step (i.e. the inlet and outlet curves revealed a similar ascending/descending shape). As previously published [44, 62-66], this behavior indicates that the particle deposition in both units was irreversible over the duration of this experiment with constant hydro-chemical conditions (i.e. flow rate, ionic strength). It is hypothesized that the high retention observed in the upper part of the sand filter may be due to a biofilm on the sand grains, which is in agreement with the results obtained from the column experiments conducted with aged sand. It has previously been shown for the same sand unit of the pilot plant used here that the bacterial density is highest at the inlet and decreases towards the outlet of the filter [67].
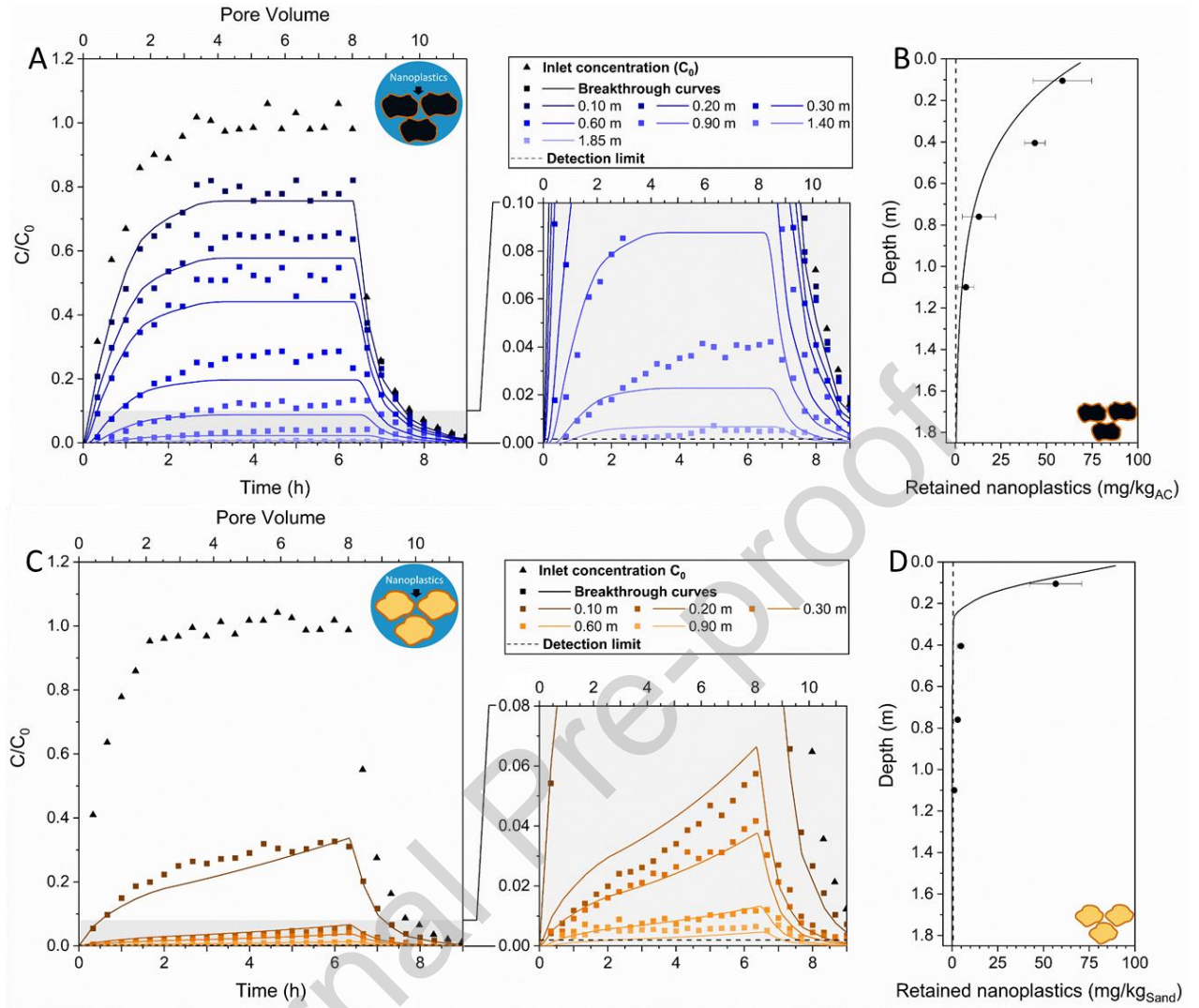
**Figure 4.** Breakthrough of NPs during pilot filtration experiments. Activated carbon (A-B): (A) Observed and modelled breakthrough curves of NPs and (B) corresponding deposition profile. Sand filter (C, D): (C) Observed and modelled breakthrough curves of NPs and (D) corresponding deposition profile. Solid lines correspond to modelled breakthrough curves and retention profiles in terms of mass of NPs. Dashed lines indicate detection limit. Triangles indicate the injected concentration of the NP detected in the water overlying the filtration media, 0.10 m above the filter. Squares indicate the $C/C_o$ values at different filter depths measured from the top to the bottom of the filter. Flow rate: 1 $m^3$/h, temperature: 6 °C, water type: ultrafiltered Lake Zurich water, filter length: 1.85 m, total experiment duration: 9h (NP injection period of 6.3 h followed by 2.7 h of NP-free lake water).

### 3.3.2 Modelling NPs in pilot-scale filtration

The particle breakthrough curves from the pilot plant were modeled using the MNMs software, which allowed an elucidation of the mechanisms controlling the transport and deposition behavior of NPs in the two filter media. By selecting the most appropriate model to fit the observed breakthrough curves, the specific attachment parameters for each filter were estimated. Due to the absence of a significant tailing in the experimental breakthrough curves, irreversible attachment kinetics were chosen for both filtration units and particle detachment was excluded. The solid lines in Fig. 4 represent the modelled depth-resolved breakthrough curves of NPs and the resulting deposition profiles along the AC (Fig. 4A and 4B) and sand (Fig. 4C and 4D) filtration units. Based on the gradual increase of NP retention with filter depth, a single homogeneous layer was used to describe the retention of NPs in the AC filtration media (Table S6). The best fit of the breakthrough curves was obtained by adopting linear irreversible attachment kinetics ($f_{att} = 1$) with an attachment coefficient ($k_a$) of 0.002 s$^{-1}$. This kinetic model assumes that the particles already deposited on the porous media had no impact on the overall attachment rate of additional particles (i.e., no blocking or ripening dynamics).

A two-layer model was required to properly describe the more complex NP breakthrough curves observed in the sand filtration unit (Table S6). The upper layer, corresponding to the first 0.2 m of the filter where a high NP retention was observed and a high bacterial density has been previously shown for this filter [67], was approximated with a dual site deposition model: linear irreversible attachment kinetics ($f_{att,1} = 1$) approximating the particle-sand interactions, and blocking irreversible attachment kinetics ($f_{att,2} = 1 - \frac{S_2}{S_{max,bio}}$) to model the particle-biofilm interactions. Single site linear irreversible attachment kinetics ($f_{att,1} = 1$) were used to model the subsequent 1.65 m of the sand filter. In agreement with previous studies [52], the attachment coefficient for the NPs-biofilm interactions ($k_{a,2} = 0.0167 \, s^{-1}$) were estimated to be almost one order of magnitude higher than the attachment coefficient

for the NPs-sand interactions ($k_{a,1} = 0.0025 \, s^{-1}$). However, the blocking model used to describe the NPs-biofilm interactions suggests that this is a time-dependent deposition process, where the attachment rate for NPs gradually decreases as particles progressively cover the biofilm layer. These models are in agreement with the shape of the experimental breakthrough curves, where we observed an increase of the NP concentration over time. Therefore, after a sufficient number of NPs have been injected into the filter covering most of the surface of the biofilm, the filter is anticipated to behave like a homogeneous sand layer with a constant attachment coefficient of $0.0025 \, s^{-1}$. The attachment coefficients of the sand are higher than those calculated for the AC, therefore NPs are expected to be more efficiently retained in the sand compared to the AC filter. This is in agreement with laboratory column experiments with the aged filter media. The retained NPs per gram of dry AC or sand at four different filtration depths is plotted as a function of distance from the top of the filter in Fig. 4B and 4D, respectively. The modeled depth retention profiles were consistent with the trends observed in the breakthrough curves. The profile along the AC filter showed an exponential decrease. This trend is typical for water treatment filtration systems filled with only one type of porous media and for a linear irreversible attachment model [41]. Conversely, the profile of the NPs deposited along the sand filter mainly followed a power law function with a very steep concentration decrease in the first 0.2 m. This characteristic profile of NP retention is in line with a biofilm coating the sand in the upper layers of the filter bed [67] and further supports the use of a two-layer model to describe the retention of NPs within the sand filter.

The experimental data shown for both the laboratory column experiments and the pilot filtration units have been obtained from short-term experiments covering less than 10 pore volumes. This timescale was sufficient for identifying and characterizing NP transport mechanisms in the filtration media but may overlook effects over extended run times, which are difficult to predict based on data from short NP injections. For

longer filter run times, the following two scenarios can be considered: (i) filter clogging and (ii) filter saturation. Filter clogging, for example with excess organic matter, particulates of all types and biofilm growth, may lead to an increased filter efficiency but would also induce an increasing head loss, which would eventually trigger backwash cycles. Backwashing removes the biofilms grown on the filtration media to some extent and it is hypothesized that the NPs attached to the biofilm would be removed as well. It is possible that this procedure may also be effective for detaching NPs from the filter substrate, reestablishing the initial filtration capacity of the filters. However, further investigations are needed to address these aspects specifically. Overall, filter clogging would trigger backwashing but would not result in a breakthrough of NPs through the filtration media.

In the case of filter saturation, NPs would break through after having entirely covered the surface of the granular media with NPs. To assess the relevant timescale for this process, we have estimated the time necessary for sand and AC filter saturation with three different inlet NP concentrations (2 mg NPs/L, similar to the column and pilot-scale experiments, and two lower concentrations of 0.2 and 0.02 mg/L; Table S7). Saturations for both AC and sand filters with the highest inlet NP concentration simulated by the MNM model were reached after 11.2 and 29.1 days, respectively. The time necessary for the saturation of the filters considerably increased when the other two lower (and likely more relevant) NP concentrations were used. The AC and sand filters with an inlet concentrations of 0.2 mg NPs/L were modeled to saturate after 111.9 and 290.5 days, respectively. Using inlet concentrations of 0.2 or 0.02 mg NPs/L would still require ~40 and ~400 days to reach 1% saturation (99% removal) of the sand filter. These times suggest that regularly scheduled backwashing cycles, typically performed weekly to once per month depending on the filter, will be conducted before reaching 1% saturation of filter media. It is also worth noting that NPs occurring in the source water may be better retained than the spherical NPs used in this study due to

an increase on the physical retention of asymmetrical and irregular NPs [68]. This would increase the retention efficiencies of NPs in filtration systems of DWTPs and, therefore, further support the suitability of the current treatment chain for removing NPs.

*3.4 Simulation of removal of NPs in a full-scale DWTP*

Interaction parameters ($k_a$, $S_{max,bio}$) extracted from modeling the breakthrough curves of the pilot plant filtration experiments were fed into the MNMs model to estimate the removal of NPs in full-scale DWTP filters. This plant operates with shorter filters and at different flow rates in comparison with the conditions used for the pilot experiments. The mean flow rate applied at each filter with their corresponding individual and cumulative removal efficiencies ($\eta$) and $\log_{10}$-removals (LRV) are shown in Fig. 5. Using a high NP inlet concentration in the feed water, similar to those used for laboratory and pilot filtration experiments as a worst-case scenario, we calculated a 58% abatement in the outlet of the rapid sand filter. This means that 0.84 mg NPs/L enter the post-treatment by AC, which retains an additional 37% of the incoming NPs. With a filtration efficiency of >99% for the slow sand filter, the concentration of NPs in the treated water after the three filtration steps decreased to 0.0005 mg NPs/L. These results indicate an overall LRV of 3.6, with the majority of the NPs retained in the slow sand filter ($LRV_3 = 3.0$). To assess the sensitivity of the filtration efficiency as a function of the flow rate, the Zurich DWTP was also simulated at the highest and lowest flow rate applied under normal operational conditions at each filtration step (Fig. S8). The results demonstrate that the removal efficiency increases with decreasing flow rate, in agreement with the observations from the column experiments. The overall LRV operating the plant at the lower flow rate was 6.8 whereas a LRV of 2.5 was obtained

for the highest flow rate. This highlights the importance of the operational parameters selected for the DWTP in controlling NP retention along the water treatment chain.
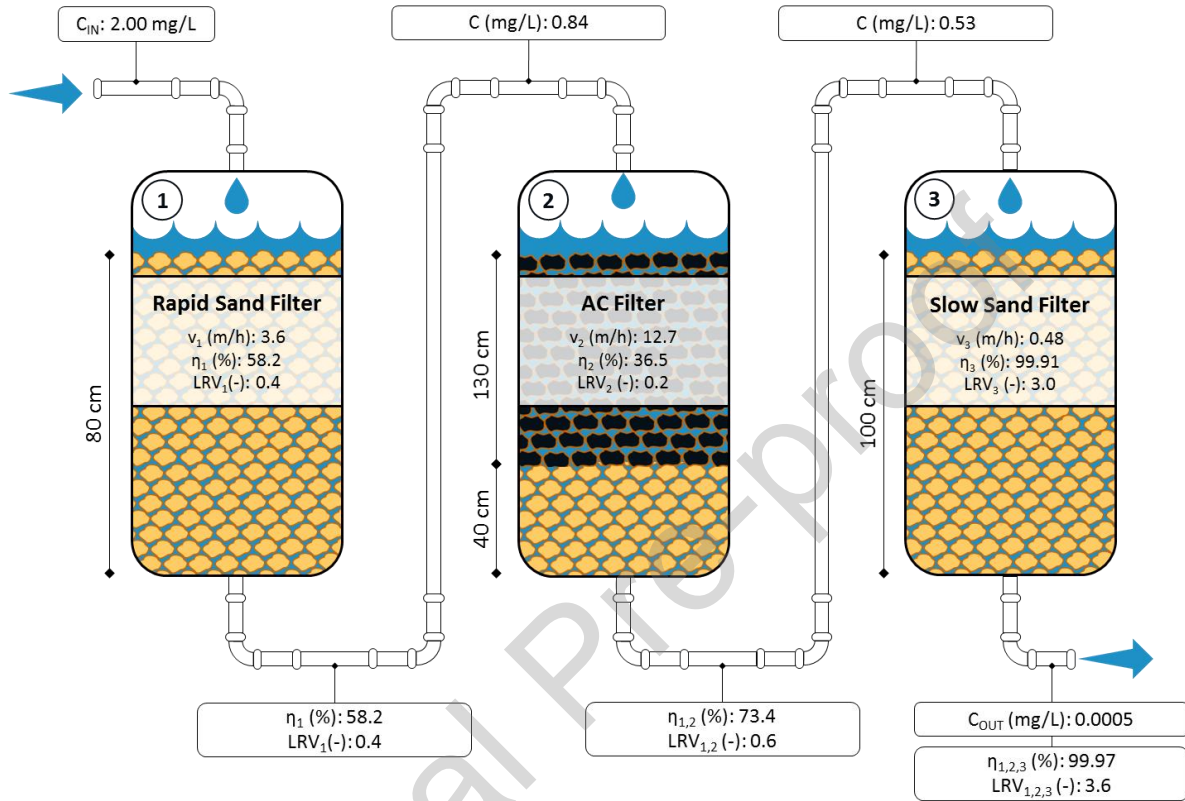


**Figure 5.** Simulation of the performance of typical DWTP, equipped with (1) a rapid sand filter, (2) AC filter (2) and (3) slow sand filter. C: concentration; $C_{IN}$: Inlet concentration; $C_{out}$: Outlet concentration; v: Flow rate; $\eta_n$: Removal efficiency; $LRV_n$: log-removal.

In agreement with previously published data [23, 25], results from this study suggest that NPs are efficiently retained in DWTPs which contain slow sand filtration units. However, DWTPs with only rapid sand filtration or a combination of rapid sand filtration with AC filtration may achieve NPs retention less than one LRV. Nevertheless, higher overall removal efficiencies can be expected in real systems. Widely applied treatment steps such as coagulation, flocculation and sedimentation likely remove NPs from suspension before they reach the filter media. In this regard, the coagulants used

during these treatments have been proven to remove NPs from suspension to some extent and to enhance their removal rate during subsequent filtration steps [23, 25]. The so-called schmutzdecke (a thick and biologically active scum layer accumulated on top of slow sand filtration units which consists of algae, bacteria, diatoms, protozoans and metazoan [55]) may also substantially improve NP removal. The schmutzdecke has proven to be highly efficient in removing many organic and inorganic compounds in full-scale DWTPs and is often considered the most effective removal compartment of slow sand filtration systems [69]. As discussed in section 3.3.2 (Modelling NPs in pilot-scale filtration), saturation of the filter would result in a breakthrough of the NPs. However, due to the continuous growth of the schmutzdecke, deposited NPs will be incorporated into the biofilm over time making a saturation of the filter unlikely. Filter clogging, which may eventually occur, is prevented by removing the top few centimeters of the slow sand filters every couple of years. A high removal rate of >99.9 % during slow sand filtration will thus be maintained of extended periods of time.

Additionally, regular backwashing cycles in the rapid sand and AC filters are key processes to take into account as they are generally performed to remove inorganic particles and excessive biomass, which prevents unacceptable head loss and maintains the finished water at a high quality. As this is a key process in DWPTs, its effectiveness for removing NPs from the filter media should be assessed in future studies. Ultrafiltration membranes are increasingly used in DWTPs [13, 31, 70] which will further help to keep the finished water free of any particulate contaminants larger than approximately 10 nm.

Water for human consumption may contain plastic particles, either when extracted groundwater or surface water is used [71]. Quantities of NPs in freshwater systems, including drinking water sources, are likely to increase in the future as a result of continued degradation and fragmentation of plastics in the environment. Despite the high removal efficiency of NPs during drinking water treatment demonstrated in this

study, the concentration of NPs entering the treatment plant needs to be considered when assessing the effectiveness of DWTPs [49]. In total, approximately 59% of the drinking water produced in Europe is slightly treated or treated only with a conventional system (i.e. rapid sand filtration and coagulation/sedimentation/filtration) [72]. Therefore, the specific configuration of DWTPs will be a key factor in determining overall NPs removal. As we have demonstrated in this study, the exceptional performance of slow sand filters to remove NPs from source water is an efficient barrier to protect drinking water from particulate contaminants, including NPs. However, due to large space requirements, slow sand filters are gradually being removed and instead ultrafiltration units are often installed as a single filtration step in newly constructed plants. With pore sizes of approximately 10 nm, high removal efficiencies of NPs are expected by such treatment processes.

## 4 Conclusions

Ozonation with ozone doses relevant for drinking water treatment had negligible impacts on NPs surface properties and barely alter their retention during subsequent filtration steps. Column experiments demonstrated the influence of operational conditions, water chemistry and filter media type in NPs filtration efficiency in different stages of drinking water treatment processes. Increasing filter length and decreasing flow rates both increased the NPs retention in the columns. The use of lake water instead of DI water reduced NPs transport through the columns, likely caused by to the compression of the electric double layer of both the NPs and the filtration media due to the higher ionic strength of the lake water. The formation of a biofilm on sand filtration media was identified as key element and increased the removal efficiency of NPs in columns experiments conducted with aged sand from 43% to 77%. In agreement with the results from the laboratory-scale experiments, NPs in the pilot filtration units were efficiently retained in the sand filter but showed less retention in the AC filter. 99.5%

and 10% of the NPs were retained in the first 0.9 m of the sand and AC filter, respectively. A full-scale DWTP including rapid and slow sand and AC filtration was modelled based on experiments from pilot and lab-scale experiments, and the results suggested a high NPs removal (> 3-$\log_{10}$ units) from lake water. Overall, slow sand filtration was dominant in retaining NPs, with approximately 3-$\log_{10}$ removal. The continuous growth of the biofilm in the slow sand filter will prevent filter saturation and thus maintain a high removal efficiency (> 99.9 %). The results presented here for removal of NPs are modeled for a specific case, the Zurich DWTP, and therefore further data from other treatment plants with different configurations are needed. In particular, specific treatment processes of a given DWTP should be considered including (1) effectiveness of coagulation processes to remove NPs before filtration, (2) suitability of backwashing cycles for removing NPs from the biofilm/filter, (3) treatment chains lacking slow sand filtration (which we found here to be the most significant removal step), (4) treatment plants including membrane filtration processes and (5) total load of NPs in the source water. The results of this study can serve as a baseline for assessing the performance of DWTPs to remove NPs from polluted water sources and the capability of current water treatment infrastructure to provide plastic-free, potable water.

## References

[1] K.L. Law, Plastics in the marine environment, Annual review of marine science, 9 (2017) 205-229.

[2] C. Li, R. Busquets, L.C. Campos, Assessment of microplastics in freshwater systems: A review, Science of the Total Environment, 707 (2020) 135578.

[3] A.A. Koelmans, N.H.M. Nor, E. Hermsen, M. Kooi, S.M. Mintenig, J. De France, Microplastics in freshwaters and drinking water: Critical review and assessment of data quality, Water research, 155 (2019) 410-422.

[4] N.B. Hartmann, T. Huffer, R.C. Thompson, M. Hassellöv, A. Verschoor, A.E. Daugaard, S. Rist, T. Karlsson, N. Brennholt, M. Cole, Are we speaking the same language? Recommendations for a definition and categorization framework for plastic debris, in, ACS Publications, 2019.

[5] S. Lambert, M. Wagner, Characterisation of nanoplastics during the degradation of polystyrene, Chemosphere, 145 (2016) 265-268.

[6] L.M. Hernandez, E.G. Xu, H.C. Larsson, R. Tahara, V.B. Maisuria, N. Tufenkji, Plastic teabags release billions of microparticles and nanoparticles into tea, Environmental science & technology, 53 (2019) 12300-12310.

[7] D.M. Mitrano, P. Wick, B. Nowack, Placing nanoplastics in the context of global plastic pollution, Nature Nanotechnology, 16 (2021) 491-500.

[8] J. Gigault, H. El Hadri, B. Nguyen, B. Grassl, L. Rowenczyk, N. Tufenkji, S. Feng, M. Wiesner, Nanoplastics are neither microplastics nor engineered nanoparticles, Nature nanotechnology, 16 (2021) 501-507.

[9] F. Rosario-Ortiz, J. Rose, V. Speight, U. Von Gunten, J. Schnoor, How do you like your tap water?, Science, 351 (2016) 912-914.

[10] C.P. Gerba, I. Pepper, Drinking water treatment, in: Environmental and Pollution Science, Elsevier, 2019, pp. 435-454.

[11] S. Mintenig, M. Löder, S. Primpke, G. Gerdts, Low numbers of microplastics detected in drinking water from ground water sources, Science of the total environment, 648 (2019) 631-635.

[12] M. Pivokonský, L. Pivokonská, K. Novotná, L. Čermáková, M. Klimtová, Occurrence and fate of microplastics at two different drinking water treatment plants within a river catchment, Science of the Total Environment, 741 (2020) 140236.

[13] Z. Wang, T. Lin, W. Chen, Occurrence and removal of microplastics in an advanced drinking water treatment plant (ADWTP), Science of the Total Environment, 700 (2020) 134520.

[14] A.C. Johnson, H. Ball, R. Cross, A.A. Horton, M.D. Jurgens, D.S. Read, J. Vollertsen, C. Svendsen, Identification and quantification of microplastics in potable water and their sources within water treatment works in England and Wales, Environmental science & technology, 54 (2020) 12326-12334.

[15] M. Pivokonsky, L. Cermakova, K. Novotna, P. Peer, T. Cajthaml, V. Janda, Occurrence of microplastics in raw and treated drinking water, Science of the total environment, 643 (2018) 1644-1651.

[16] S.A. Parsons, B. Jefferson, Introduction to potable water treatment processes, Wiley Online Library, 2006.

[17] S. Tripathi, D. Champagne, N. Tufenkji, Transport behavior of selected nanoparticles with different surface coatings in granular porous media coated with Pseudomonas aeruginosa biofilm, Environmental science & technology, 46 (2012) 6942-6949.

[18] Z. Li, A.A. Hassan, E. Sahle-Demessie, G.A. Sorial, Transport of nanoparticles with dispersant through biofilm coated drinking water sand filters, Water research, 47 (2013) 6457-6466.

[19] M.R. Mitzel, S. Sand, J.K. Whalen, N. Tufenkji, Hydrophobicity of biofilm coatings influences the transport dynamics of polystyrene nanoparticles in biofilm-coated sand, Water research, 92 (2016) 113-120.

[20] J.L. Hoggan, D.A. Sabatini, T.C. Kibbey, Transport and retention of TiO2 and polystyrene nanoparticles during drainage from tall heterogeneous layered columns, Journal of contaminant hydrology, 194 (2016) 30-35.

[21] S.A. Bradford, S.R. Yates, M. Bettahar, J. Simunek, Physical factors affecting the transport and fate of colloids in saturated porous media, Water resources research, 38 (2002) 63-61-63-12.

[22] M. Velimirovic, C. Bianco, N. Ferrantello, T. Tosco, A. Casasso, R. Sethi, D. Schmid, S. Wagner, K. Miyajima, N. Klaas, A large-scale 3D study on transport of humic acid-coated goethite nanoparticles for aquifer remediation, Water, 12 (2020) 1207.

[23] L.R. Arenas, S.R. Gentile, S. Zimmermann, S. Stoll, Fate and removal efficiency of polystyrene nanoplastics in a pilot drinking water treatment plant, Science of the Total Environment, 813 (2022) 152623.

[24] L.R. Arenas, S.R. Gentile, S. Zimmermann, S. Stoll, Nanoplastics adsorption and removal efficiency by granular activated carbon used in drinking water treatment process, Science of the Total Environment, 791 (2021) 148175.

[25] Y. Zhang, A. Diehl, A. Lewandowski, K. Gopalakrishnan, T. Baker, Removal efficiency of micro-and nanoplastics (180 nm–125 μm) during drinking water treatment, Science of the Total Environment, 720 (2020) 137383.

[26] A.S. Keller, J. Jimenez-Martinez, D.M. Mitrano, Transport of nano-and microplastic through unsaturated porous media from sewage sludge application, Environmental science & technology, 54 (2019) 911-920.

[27] D.M. Mitrano, A. Beltzung, S. Frehland, M. Schmiedgruber, A. Cingolani, F. Schmidt, Synthesis of metal-doped nanoplastics and their utility to investigate fate and behaviour in complex environmental systems, Nature nanotechnology, 14 (2019) 362-368.

[28] S. Frehland, R. Kaegi, R. Hufenus, D.M. Mitrano, Long-term assessment of nanoplastic particle and microplastic fiber flux through a pilot wastewater treatment plant using metal-doped plastics, Water Research, 182 (2020) 115860.

[29] C. Bianco, T. Tosco, R. Sethi, A 3-dimensional micro-and nanoparticle transport and filtration model (MNM3D) applied to the migration of carbon-based nanomaterials in porous media, Journal of contaminant hydrology, 193 (2016) 10-20.

[30] C. Bianco, J.E.P. Higuita, T. Tosco, A. Tiraferri, R. Sethi, Controlled deposition of particles in porous media for effective aquifer nanoremediation, Scientific reports, 7 (2017) 1-10.

[31] M. Bourgin, E. Borowska, J. Helbing, J. Hollender, H.-P. Kaiser, C. Kienle, C.S. McArdell, E. Simon, U. Von Gunten, Effect of operational and water quality parameters on conventional ozonation and the advanced oxidation process O3/H2O2: kinetics of micropollutant abatement, transformation product and bromate formation in a surface water, Water research, 122 (2017) 234-245.

[32] H. Bader, J. Hoigné, Determination of ozone in water by the indigo method, Water research, 15 (1981) 449-456.

[33] C. von Sonntag, U. von Gunten, Chemistry of ozone in water and wastewater treatment, IWA publishing, 2012.

[34] F. Hammes, C. Berger, O. Köster, T. Egli, Assessing biological stability of drinking water without disinfectant residuals in a full-scale water supply system, Journal of Water Supply: Research and Technology—AQUA, 59 (2010) 31-40.

[35] U. von Gunten, J. Zobrist, Biogeochemical changes in groundwater-infiltration systems: column studies, Geochimica et Cosmochimica Acta, 57 (1993) 3895-3906.

[36] J.M. Farner, J. De Tommaso, H. Mantel, R.S. Cheong, N. Tufenkji, Effect of freeze/thaw on aggregation and transport of nano-TiO 2 in saturated porous media, Environmental Science: Nano, 7 (2020) 1781-1793.

[37] J.C. Crittenden, R.R. Trussell, D.W. Hand, K. Howe, G. Tchobanoglous, MWH's water treatment: principles and design, John Wiley & Sons, 2012.

[38] K. Lautenschlager, C. Hwang, F. Ling, W.-T. Liu, N. Boon, O. Köster, T. Egli, F. Hammes, Abundance and composition of indigenous bacterial communities in a multi-step biofiltration-based drinking water treatment plant, Water Research, 62 (2014) 40-52.

[39] F. Mondino, A. Piscitello, C. Bianco, A. Gallo, A. de Folly D'Auris, T. Tosco, M. Tagliabue, R. Sethi, Injection of zerovalent iron gels for aquifer nanoremediation: Lab experiments and modeling, Water, 12 (2020) 826.

[40] A. Beryani, M.R.A. Moghaddam, T. Tosco, C. Bianco, S.M. Hosseini, E. Kowsari, R. Sethi, Key factors affecting graphene oxide transport in saturated porous media, Science of The Total Environment, 698 (2020) 134224.

[41] N. Tufenkji, M. Elimelech, Deviation from the classical colloid filtration theory in the presence of repulsive DLVO interactions, Langmuir, 20 (2004) 10818-10828.

[42] F. Messina, D.L. Marchisio, R. Sethi, An extended and total flux normalized correlation equation for predicting single-collector efficiency, Journal of colloid and interface science, 446 (2015) 185-193.

[43] S. Sasidharan, S. Torkzaban, S.A. Bradford, P.J. Dillon, P.G. Cook, Coupled effects of hydrodynamic and solution chemistry on long-term nanoparticle transport and deposition in saturated porous media, Colloids and Surfaces A: Physicochemical and Engineering Aspects, 457 (2014) 169-179.

[44] T. Tosco, A. Tiraferri, R. Sethi, Ionic strength dependent transport of microparticles in saturated porous media: Modeling mobilization and immobilization phenomena under transient chemical conditions, Environmental science & technology, 43 (2009) 4425-4431.

[45] J. Liu, T. Zhang, L. Tian, X. Liu, Z. Qi, Y. Ma, R. Ji, W. Chen, Aging significantly affects mobility and contaminant-mobilizing ability of nanoplastics in saturated loamy sand, Environmental science & technology, 53 (2019) 5805-5815.

[46] L. Tian, B. Kolvenbach, N. Corvini, S. Wang, N. Tavanaie, L. Wang, Y. Ma, S. Scheu, P.F.-X. Corvini, R. Ji, Mineralisation of 14C-labelled polystyrene plastics by Penicillium variabile after ozonation pre-treatment, New biotechnology, 38 (2017) 101-105.

[47] D. Teare, N. Emmison, C. Ton-That, R. Bradley, Cellular attachment to ultraviolet ozone modified polystyrene surfaces, Langmuir, 16 (2000) 2818-2824.

[48] E.A. Abdulal, A. Khot, A. Bailey, M. Mehan, T. Debies, G.A. Takacs, Surface characterization of polystyrene treated with ozone and grafted with poly (acrylic acid), Journal of Adhesion Science and Technology, 29 (2015) 1-11.

[49] J. Hou, M. Zhang, P. Wang, C. Wang, L. Miao, Y. Xu, G. You, B. Lv, Y. Yang, Z. Liu, Transport and long-term release behavior of polymer-coated silver nanoparticles in saturated quartz sand: The impacts of input concentration, grain size and flow rate, Water research, 127 (2017) 86-95.

[50] X. Jiang, X. Wang, M. Tong, H. Kim, Initial transport and retention behaviors of ZnO nanoparticles in quartz sand porous media coated with Escherichia coli biofilm, Environmental pollution, 174 (2013) 38-49.

[51] A.R. Esfahani, O. Batelaan, J.L. Hutson, H.J. Fallowfield, Transport and retention of graphene oxide nanoparticles in sandy and carbonaceous aquifer sediments: Effect of physicochemical factors and natural biofilm, Journal of Environmental Management, 278 (2021) 111419.

[52] M.R. Mitzel, N. Tufenkji, Transport of industrial PVP-stabilized silver nanoparticles in saturated quartz sand coated with Pseudomonas aeruginosa PAO1 biofilm of variable age, Environmental science & technology, 48 (2014) 2715-2723.

[53] S. Velten, F. Hammes, M. Boller, T. Egli, Rapid and direct estimation of active biomass on granular activated carbon through adenosine tri-phosphate (ATP) determination, Water Research, 41 (2007) 1973-1983.

[54] M. Vignola, D. Werner, M.J. Wade, P. Meynet, R.J. Davenport, Medium shapes the microbial community of water filters with implications for effluent quality, Water research, 129 (2018) 499-508.

[55] S. Oh, F. Hammes, W.-T. Liu, Metagenomic characterization of biofilter microbial communities in a full-scale drinking water treatment plant, Water Research, 128 (2018) 278-285.

[56] I. Chowdhury, Y. Hong, R.J. Honda, S.L. Walker, Mechanisms of TiO2 nanoparticle transport in porous media: Role of solution chemistry, nanoparticle concentration, and flowrate, Journal of colloid and interface science, 360 (2011) 548-555.

[57] G. Chen, X. Liu, C. Su, Transport and retention of TiO2 rutile nanoparticles in saturated porous media under low-ionic-strength conditions: measurements and mechanisms, Langmuir, 27 (2011) 5393-5402.

[58] A. Tiraferri, L.A.S. Hernandez, C. Bianco, T. Tosco, R. Sethi, Colloidal behavior of goethite nanoparticles modified with humic acid and implications for aquifer reclamation, Journal of Nanoparticle Research, 19 (2017) 107.

[59] A.J. Pelley, N. Tufenkji, Effect of particle size and natural organic matter on the migration of nano-and microscale latex particles in saturated porous media, Journal of colloid and interface science, 321 (2008) 74-83.

[60] H.-P. Kaiser, O. Köster, M. Gresch, P.M. Périsset, P. Jäggi, E. Salhi, U. Von Gunten, Process control for ozonation systems: a novel real-time approach, Ozone: science & engineering, 35 (2013) 168-185.

[61] C.-H. Ko, M. Elimelech, The "shadow effect" in colloid transport and deposition dynamics in granular porous media: measurements and mechanisms, Environmental science & technology, 34 (2000) 3681-3689.

[62] G. Cornelis, L. Pang, C. Doolette, J.K. Kirby, M.J. McLaughlin, Transport of silver nanoparticles in saturated columns of natural soils, Science of the Total Environment, 463 (2013) 120-130.

[63] T. Tosco, J. Bosch, R.U. Meckenstock, R. Sethi, Transport of ferrihydrite nanoparticles in saturated porous media: role of ionic strength and flow rate, Environmental science & technology, 46 (2012) 4008-4015.

[64] T. Raychoudhury, N. Tufenkji, S. Ghoshal, Straining of polyelectrolyte-stabilized nanoscale zero valent iron particles during transport through granular porous media, Water research, 50 (2014) 80-89.

[65] I.L. Molnar, W.P. Johnson, J.I. Gerhard, C.S. Willson, D.M. O'carroll, Predicting colloid transport through saturated porous media: A critical review, Water Resources Research, 51 (2015) 6804-6845.

[66] M. Tong, X. Li, C.N. Brow, W.P. Johnson, Detachment-influenced transport of an adhesion-deficient bacterial strain within water-reactive porous media, Environmental Science & Technology, 39 (2005) 2500-2508.

[67] R. Gulde, B. Clerc, M. Rutsch, J. Helbing, E. Salhi, C.S. McArdell, U. von Gunten, Oxidation of 51 micropollutants during drinking water ozonation: Formation of transformation products and their fate during biological post-filtration, Water Research, (2021) 117812.

[68] A. Pradel, H. El Hadri, C. Desmet, J. Ponti, S. Reynaud, B. Grassl, J. Gigault, Deposition of environmentally relevant nanoplastic models in sand during transport experiments, Chemosphere, 255 (2020) 126912.

[69] K.R. Pfannes, K.M. Langenbach, G. Pilloni, T. Stührmann, K. Euringer, T. Lueders, T.R. Neu, J.A. Müller, M. Kästner, R.U. Meckenstock, Selective elimination of bacterial faecal indicators in the Schmutzdecke of slow sand filtration columns, Applied microbiology and biotechnology, 99 (2015) 10323-10332.

[70] W. Gao, H. Liang, J. Ma, M. Han, Z.-l. Chen, Z.-s. Han, G.-b. Li, Membrane fouling control in ultrafiltration technology for drinking water production: A review, Desalination, 272 (2011) 1-8.

[71] M. Wagner, S. Lambert, Freshwater microplastics: emerging environmental contaminants?, Springer Nature, 2018.

[72] J.P. van der Hoek, C. Bertelkamp, A. Verliefde, N. Singhal, Drinking water treatment technologies in Europe: state of the art–challenges–research needs, Journal of Water Supply: Research and Technology—AQUA, 63 (2014) 124-130.

## CRediT authorship contribution statement

**Gerardo Pulido-Reyes:** Project administration, investigation, data curation, writing original draft, **Leonardo Magherini:** Investigation, writing, modelling and simulation, review & editing, **Carlo Bianco:** Investigation, writing, modelling and simulation, review & editing, **Rajandrea Sethi:** Investigation, writing, modelling and simulation, review & editing **Urs von Gunten:** Conceptualization, resources, writing, review & editing, **Ralf Kaegi:** Funding acquisition, conceptualization, project administration, writing, review & editing **Denise M. Mitrano:** Funding acquisition, conceptualization, writing, review & editing

**Environmental implications**

Results from laboratory and pilot scale experiments using metal-labelled nanoplastic particles (NPs) indicate an efficient removal of NPs during conventional treatments of drinking water. Slow sand filtration was the most effective treatment with a NPs removal efficiency > 99.9%. The formation of a biofilm in the sand filter played a key role in removing NPs from the feed water. The results from this study can be used to estimate the degree of NPs retention in drinking water plants using similar process schemes.

**Declaration of competing interest**

☒ The authors declare that they have no known competing financial interests or personal relationships that could have appeared to influence the work reported in this paper.

☐ The authors declare the following financial interests/personal relationships which may be considered as potential competing interests:

## Graphical Abstract

**Removal of nanoplastics during typical drinking water treatment processes**
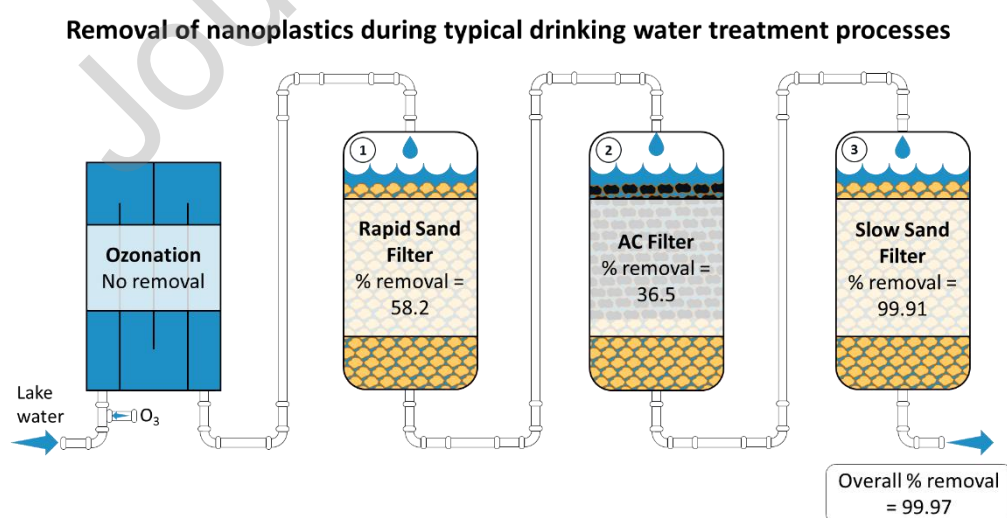
## Highlights

- Nanoplastic particles (NPs) were retained by biofilms during rapid and slow sand filtration.
- Ozonation does not affect the retention of NPs during drinking water treatment.
- 99.5% of the NPs were retained in the first 0.9 m of the pilot-scale sand filter.
- Slow sand filtration was the most effective process for removing NPs from the feed water.
- A removal efficiency of 3.6-log units was modeled for 3 consecutive filtration steps.